

## Structure and electronic properties of Fe–Ti thin films

K. SMARDZ<sup>1</sup>, L. SMARDZ<sup>2\*</sup>

<sup>1</sup>Institute of Materials Science and Engineering, Poznań University of Technology,  
pl. M. Skłodowskiej-Curie 5, 60-965 Poznań, Poland

<sup>2</sup>Institute of Molecular Physics, Polish Academy of Sciences,  
M. Smoluchowskiego 17, 60-179 Poznań, Poland

Fe/Ti multilayers (MLs) were prepared on glass substrates using UHV RF/DC magnetron sputtering. The results showed a significant drop in coercivity measured for the Fe/Ti MLs with decreasing Fe layer thickness, typically from  $H_c \approx 2.2$  kA/m to  $H_c \approx 0.2$  kA/m, observed at a critical Fe thickness of  $d_{\text{crit}} \approx 2.3$  nm. Structural studies showed that the deposition of a 0.18 nm Fe/0.22 nm Ti ML at 285 K leads to the formation of a uniform amorphous Fe–Ti alloy thin film due to strong interdiffusion during growth. On the other hand, *in situ* annealing of this ML at 750 K for 2 h resulted in the creation of a nanocrystalline phase. Furthermore, *in situ* XPS studies showed that the valence band of the nanocrystalline Fe–Ti alloy film is broader than that measured for the amorphous phase with the same average composition.

Key words: *magnetic multilayers; electronic structure*

### 1. Introduction

Metallic multilayers (MLs) composed of alternating sublayers of ferromagnetic and non-magnetic metals exhibit interesting magnetic properties which can be tailored by varying the compositions and thicknesses of the sublayers. In previous papers [1–4], we have shown that below the critical Co or Fe thickness ( $d_{\text{crit}}$ ), Co/Zr ( $d_{\text{crit}} \approx 2.8$  nm) [1], Co/Ti ( $d_{\text{crit}} \approx 3$  nm) [2, 3], and Fe/Zr ( $d_{\text{crit}} \approx 2.3$  nm) [4] MLs are magnetically soft and exhibit a saturation magnetisation higher than that observed in conventional soft magnetic films. It has been found that Co (Fe) sublayers grow in the soft magnetic nanocrystalline structure up to  $d_{\text{crit}}$  [1–4]. Above  $d_{\text{crit}}$ , Co (Fe) sublayers grow in the polycrystalline structure with an average grain size greater than the magnetic exchange length [5]. On the other hand, it is well known that a suitable annealing of

---

\*Corresponding author, e-mail: smardz@ifmpan.poznan.pl

Fe/Ti MLs leads to the formation of an amorphous phase due to a solid-state reaction [6]. Therefore, the spontaneous formation of a quasi-amorphous or nanocrystalline interface Fe–Ti alloy layer is very likely to proceed during the deposition of the Fe/Ti/Fe trilayer and especially Fe/Ti MLs. This is also consistent with the results of our structural and magnetisation studies for very similar systems Co/Ti, Co/Zr, and Fe/Zr MLs [1–4]. In this paper, we study the stability range of the polycrystalline and soft magnetic nanocrystalline iron phase as a function of the sublayer thickness. Furthermore, we study the valence band of *in situ* prepared amorphous and nanocrystalline Fe–Ti alloy thin films.

## 2. Experimental

Fe/Ti MLs were prepared on glass substrates at 285 K using computer-controlled ultra high vacuum (UHV) magnetron co-sputtering. Fe and Ti targets were sputtered using the DC and RF modes, respectively. The base pressure before deposition was lower than  $5 \times 10^{-10}$  mbar. The chemical composition and the purity of all layers was checked *in situ*, immediately after deposition, after transferring the samples to an UHV ( $4 \times 10^{-11}$  mbar) analysis chamber equipped with X-ray photoelectron spectroscopy (XPS). The XPS spectra were recorded with  $\text{AlK}_\alpha$  radiation (1486.6 eV) at room temperature using a SPECS EA 10 PLUS energy spectrometer. All emission spectra were recorded immediately after *in situ* sample transfer to a vacuum of  $8 \times 10^{-11}$  mbar. The deposition rates of Fe and Ti were checked individually with a quartz thickness monitor. The thicknesses of individual sublayers were controlled mainly by varying their deposition times. The number of repetitions was increased with decreasing Fe and Ti sublayer thicknesses, so as to keep the total thickness of the samples at about 50 nm and 500 nm for magneto-optical measurements and X-ray diffraction studies, respectively.

The Fe/Ti MLs were prepared with either wedged Fe or wedged Ti sublayers. Wedge-shaped Fe or Ti sublayers with a slope of 0.05–0.125 nm/mm were grown by moving a shutter linearly or step-wise in front of the substrate during deposition. The structures of the samples with step-like wedge forms (areas with Fe and Ti sublayers of constant thickness) were examined *ex-situ* by standard  $\theta$ – $2\theta$  X-ray diffraction (XRD) using  $\text{CuK}_\alpha$  radiation. The modulation wavelength was determined from the spacing between satellite peaks in low-angle XRD patterns. The results were consistent with the values obtained by dividing the total thickness by the number of repetitions. The thicknesses of the individual Fe and Ti sublayers were also determined using X-ray fluorescence analysis (XRF). The magnetic characterisation of the wedged Fe/Ti MLs was carried out utilizing the magneto-optical Kerr effect at room temperature. The coercive fields ( $H_c$ ) were determined from in-plane hysteresis loop measurements.

### 3. Results and discussion

The composition modulation of Fe/Ti MLs was confirmed in low-angle XRD measurements. We have observed from two to six satellite peaks for MLs with the thinner and the thicker sublayers, respectively. The wavelengths of modulation calculated from these peaks were in agreement with values determined from XRF measurements. Figure 1a shows an example of a low-angle XRD pattern for the 1.8 nm Fe/2.2 nm Ti ML. The intense satellite peaks up to the 4th order revealed the good quality of the multilayered sample. For the Fe/Ti MLs with  $d_{\text{Fe}} > 2.3$  nm and  $d_{\text{Ti}} > 2.3$  nm, high-angle X-ray diffraction patterns show the (110) and (002) reflections of bcc Fe and hcp Ti, respectively. The average Fe and Ti crystallite sizes in directions perpendicular to the substrates, as determined from the Scherer equation, are comparable to their respective sublayer thicknesses. Only very weak and broad peaks related to Fe and Ti sublayers were observed for MLs with  $d_{\text{Fe}} < 2.3$  nm and  $d_{\text{Ti}} = 2.2$  nm, in agreement with the X-ray diffraction studies reported in Ref. [3]. We have previously observed a very similar growth mode for Co sublayers in Co/Zr MLs [1]. The very broad and weak Fe and Ti reflections observed for  $d_{\text{Fe}} < \sim 2.3$  nm can be explained by the nanocrystalline growth of the sublayers (average grain size  $D \ll 10$  nm), similar to that observed earlier for Co [1–3] and Fe [4] sublayers.

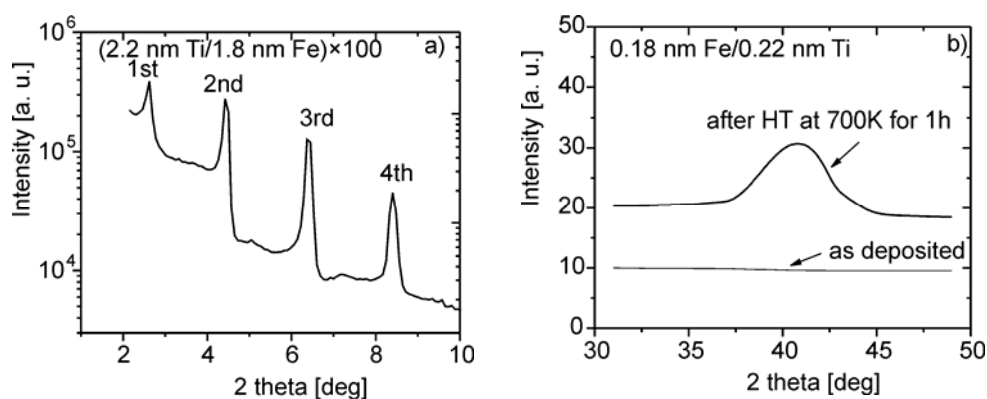


Fig. 1. Low-angle X-ray diffraction patterns ( $\text{CuK}\alpha$ ) for the 2.2 nm Ti/1.8 nm Fe multilayer (a) and high-angle X-ray diffraction patterns ( $\text{CuK}\alpha$ ) for the as deposited and annealed 0.18 nm Fe/0.22 nm Ti multilayer (b)

The above behaviour was revealed by UHV STM measurements of the average in-plane grain sizes, similar to the effect observed earlier for Co/Ti MLs [3]. Furthermore, the deposition of a 0.18 nm Fe/0.22 nm Ti ML at 285 K leads to the formation of a uniform amorphous Fe–Ti alloy thin film due to strong interdiffusion during growth. On the other hand, *in situ* annealing of the 0.18 nm Fe/0.22 nm Ti ML at 700 K for 1 h resulted in the creation of a nanocrystalline phase. The corresponding XRD patterns are shown in Fig. 1a. The average crystallite size of the FeTi alloy film,

as determined from the FWHM of the peak shown in Fig. 1b using the Scherer equation, was about 8 nm.

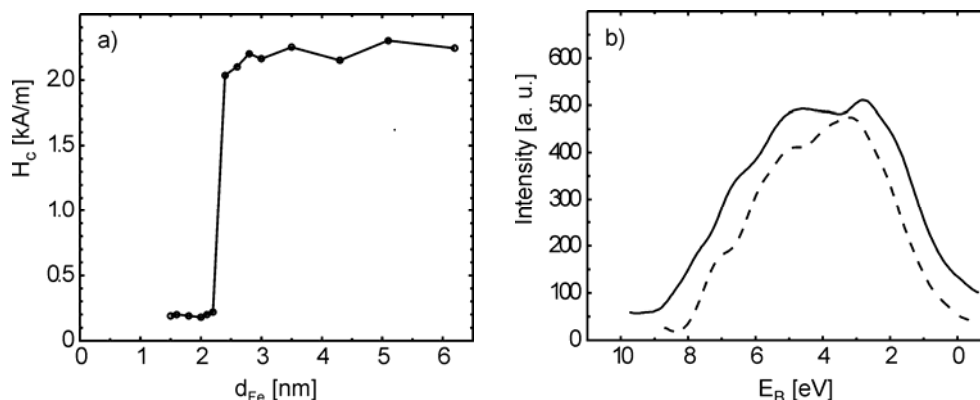


Fig. 2. Coercive field ( $H_c$ ) as a function of the Fe sublayer thickness for wedged Fe/Ti multilayers with  $d_{\text{Ti}} = 2.2$  nm (a) and XPS spectra of the as deposited (broken line) and *in situ* annealed, at 700 K for 1 h (solid line), 0.18 nm Fe/0.22 nm Ti multilayer (b)

Figure 2a shows the  $H_c$  values measured at room temperature as function of Fe sublayer thickness for wedged Fe/Ti MLs with  $d_{\text{Ti}} = 2.2$  nm. A significant drop in coercivity with decreasing Fe layer thickness – typically from  $H_c \approx 2.2$  kA/m to  $H_c \approx 0.2$  kA/m – can be observed at a critical Fe thickness of  $d_{\text{crit}} \approx 2.3$  nm. The behaviour of coercivity shown in Fig. 2a can be associated with structural properties of the Fe layer grown on Ti, similarly to the transition observed earlier for Co/Zr [2] and Co/Ti [3] MLs. According to the above interpretation, iron sublayers grow in the soft magnetic nanocrystalline phase ( $D \ll 10$  nm) for thicknesses lower than the critical one. In this case, the average Fe grain size is significantly smaller than the magnetic exchange length [5] for the iron layer ( $L_{\text{ex}} \approx 15$  nm) [5]. For thicknesses larger than  $d_{\text{crit}}$ , Fe sublayers undergo a structural transition to the polycrystalline phase with an average grains size  $D > 15$  nm [5].

Figure 2b shows the XPS valence bands of the as prepared (amorphous phase) and annealed (nanocrystalline phase) 0.18 nm Fe/0.22 nm Ti MLs. XPS measurements were performed *in situ* on freshly prepared samples with thicknesses of about 500 nm. The results showed that the valence band of the “as prepared” amorphous Fe–Ti alloy film (broken line) is broader than that measured for the polycrystalline bulk material [7]. On the other hand, the valence band of the nanocrystalline Fe–Ti alloy (solid line) is even broader than the valence band of the amorphous alloy (broken line). This is probably due to a strong deformation of the nanocrystals. Normally, the interior of the nanocrystal is constrained and the distances between atoms located at grain boundaries expanded [1, 7]. Strong modifications of the electronic structure of nanocrystalline Fe–Ti alloy films could also significantly influence their hydrogenation properties [7]. According to existing semi-empirical models [8, 9] which can explain the

maximum hydrogen absorption capacity of the metallic matrices, the significant broadening of their valence bands is a very important factor, leading to an increase in hydrogen absorption. Such behaviour has already been observed in the case of mechanically alloyed nanocrystalline FeTi- [7] and LaNi<sub>5</sub>-type[10] bulk alloys.

In the XPS experiment, we have also studied the growth of a Fe layer on a 10 nm Ti underlayer and the growth of a Ti layer on a 10 nm Fe underlayer. The freshly deposited 10 nm Ti/*d*<sub>0</sub> Fe or 10 nm Fe/*d*<sub>0</sub> Ti bilayer was transferred *in situ* from the preparation chamber to the analysis chamber, where the XPS Fe-2p<sub>3/2</sub> and Ti-3d<sub>5/2</sub> core level spectra were immediately recorded in a vacuum of 8×10<sup>-11</sup> mbar. The bilayer was then transferred back to the preparation chamber and the deposition process of the overlayer was continued. From the exponential variation of the XPS Fe-2p and Ti-3d integral intensities with increasing layer thickness, we conclude that the Fe and Ti sublayers grow homogeneously [11, 12].

In conclusion, the planar growth of Fe and Ti sublayers was confirmed *in situ* by XPS. Iron sublayers grow on sufficiently thick titanium sublayers in the soft magnetic nanocrystalline phase up to a critical thickness of *d*<sub>crit</sub> ≈ 2.3 nm. *In situ* XPS studies showed that the valence band of the Fe–Ti alloy thin film strongly depends on its microstructure.

#### Acknowledgements

This work was financially supported by the Polish Committee for Scientific Research under grant No. PBZ KBN 044/P03/02 2001.

#### References

- [1] SMARDZ L., LE DANG K., NIEDOBA H., CHRZUMNICKA K., J. Magn. Magn. Mater., 140–144 (1995), 569.
- [2] SMARDZ L., Sol. State Comm., 112 (1999), 693.
- [3] SMARDZ L., SMARDZ K., CZAJKA R., Cryst. Res. Technol., 36 (2001), 1019.
- [4] SMARDZ L., J. All. Comp., 395 (2005), 17.
- [5] HERZER G., J. Magn. Magn. Mater., 157/158 (1996), 133.
- [6] STOBIECKI T., KOPCEWICZ M., CASTAÑO F. J., Chaos, Solitons and Fractals, 10 (1999), 2031.
- [7] SMARDZ K., SMARDZ L., JURCZYK M., JANKOWSKA E., Phys. Stat. Sol. A, 196 (2003), 263.
- [8] BOUTEN P. C., MIEDEMA A. R., J. Less Common Metals, 71 (1980), 147.
- [9] GRIESSEN R., Phys. Rev., B38 (1988), 3690.
- [10] SMARDZ L., SMARDZ K., NOWAK M., JURCZYK M., Cryst. Res. Technol., 36 (2001), 1385.
- [11] SMARDZ L., SMARDZ K., Mol. Phys. Rep., 40 (2004), 137.
- [12] BRIGGS D., [in:] *Handbook of X-ray and Ultraviolet Photoelectron Spectroscopy*, D. Briggs (Ed.), Heyden and Son Ltd., London, 1977, p. 153 and references therein.

Received 1 June 2005

Revised 10 October 2005